ACS OMEGA

Open Access

http://pubs.acs.org/journal/acsodf

Article

Strategies to Enhance L-Isoleucine Synthesis by Modifying the Threonine Metabolism Pathway in *Escherichia coli*

HaoJie Zhang, Tong Ye, Liu Fengmin, Xiangjun Zhang, Jipeng Wang, Xiaobo Wei, Yun Ping Neo, Huiyan Liu, and Haitian Fang*

Cite This: *ACS Omega* 2024, 9, 10276−10285

Read Online

ACCESS | Metrics & More | Article Recommendations | Supporting Information

ABSTRACT: L-threonine as an important precursor substance of L-isoleucine and improving its accumulation in *Escherichia coli* became an important idea to construct a chassis strain with high L-isoleucine production. Meanwhile, the effect of L-threonine metabolic pathway disruption in *E. coli* for the improved production of L-isoleucine remains unrevealed. In the present study, a mutant strain of *E. coli* was engineered by inactivating specific metabolic pathways (e.g., Δ*tdh*, Δ*ltaE*, and Δ*yiaY*) that were associated with L-threonine metabolism but unrelated to L-isoleucine synthesis. This was done with the aim to reduce the breakdown of L-threonine and, thereby, increase the production of L-isoleucine. The results obtained demonstrated a 72.3% increment in L-isoleucine production from 4.34 to 7.48 g·L^{-1} in the mutant strain compared with the original strain, with an unexpected 10.3% increment in bacterial growth as measured at OD_{600}. Transcriptome analysis was also conducted on both the mutant strain NXU102 and the original strain NXU101 in the present study to gain a comprehensive understanding of their physiological attributes. The findings revealed a notable disparity in 1294 genes between the two strains, with 658 genes exhibiting up-regulation and 636 genes displaying down-regulation. The activity of tricarboxylic acid (TCA) cycle-related genes was found to decrease, but oxidative phosphorylation-related genes were highly up-regulated, which explained the increased activity of the mutant strain. For instance, L-lysine catabolism-related genes were found to be up-regulated, which reconfigured the carbon flow into the TCA cycle. The augmentation of acetic acid degradation pathway-related genes assisted in the reduction in acetic acid accumulation that could retard cell growth. Notably, substantial up-regulation of the majority of genes within the aspartate pathway could potentially account for the increased production of L-isoleucine in the present study. In this paper, a chassis strain with an L-isoleucine yield of 7.48 g·L^{-1} was successfully constructed by cutting off the threonine metabolic pathway. Meanwhile, transcriptomic analysis revealed that the cutting off of the threonine metabolic pathway induced perturbation of genes related to the pathways associated with the synthesis of L-isoleucine, such as the tricarboxylic acid cycle, glycolysis, and aspartic acid pathway.

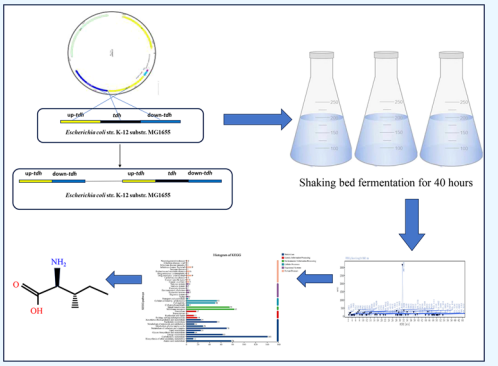

INTRODUCTION

L-isoleucine is referred to as a branched chain amino acid together with L-valine and L-leucine. It is a high-value-added amino acid with muscle repair function, which is also often used to treat cirrhosis, obesity, coma, and other conditions.[1−4] L-isoleucine has received much attention in recent years as a synthetic precursor for the antiglycolytic drug 4-hydroxyisoleucine.[5,6] Fermentation is the primary method for industrial production of L-isoleucine; meanwhile, chemical synthesis and extraction from hair also play a key role in its production.[7−9] Additionally, metabolic engineering of the L-isoleucine biosynthesis pathway in *Corynebacterium glutamicum* and *E. coli* has also been widely used for the industrial production of this amino acid.

As highlighted earlier, *E. coli* has been used for the production of L-isoleucine. Figure 1 shows the biosynthesis pathway, regulatory mechanism, and transport system of L-isoleucine in *E. coli*. Briefly, glucose will undergo a series of reactions to generate aspartic acid, followed by L-aspartic acid being sequentially converted to L-threonine through a five-step enzymatic reaction catalyzed by L-aspartate kinase (AK), aspartate semialdehyde dehydrogenase (ASD), high serine dehydrogenase (HDH), high serine kinase (HSK), and threonine synthase (TS). L-threonine is transformed into L-isoleucine via another five-step enzymatic reaction catalyzed by threonine dehydratase encoded by *ilvA*. In order to increase the accumulation of L-isoleucine, it becomes particularly important to attenuate the metabolism of its important precursor, L-threonine (Figure 1).

Received: October 2, 2023
Revised: January 23, 2024
Accepted: January 30, 2024
Published: February 22, 2024

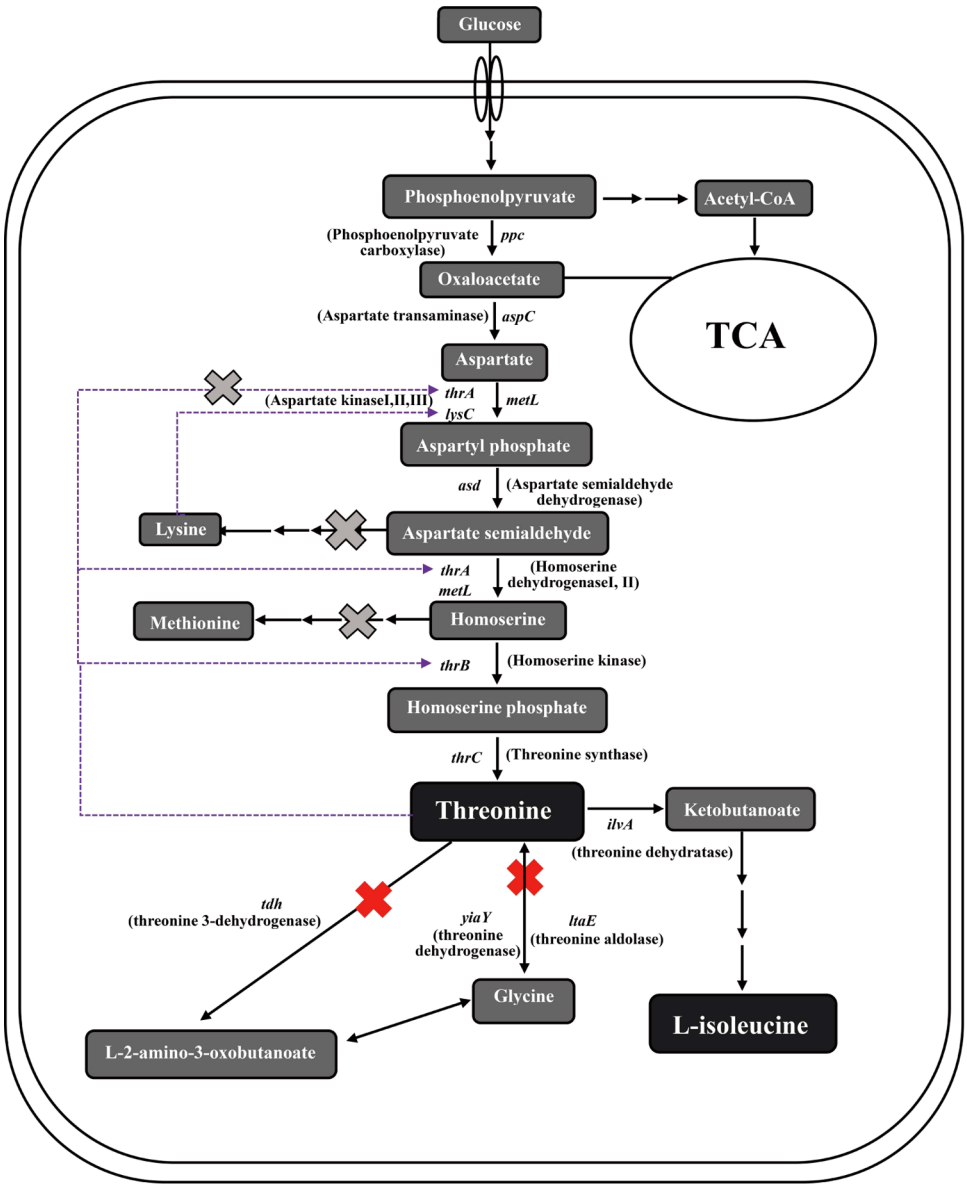

Figure 1. L-isoleucine biosynthetic pathway in *E. coli* and strain modification idea/background.

At present, there are three established pathways for the degradation of threonine within *E. coli* cells. These three genes are *tdh*, which is responsible for encoding threonine 3-dehydrogenase, *ltaE*, which is responsible for encoding threonine aldolase, and *yiaY*, which is responsible for encoding L-threonine dehydrogenase. Notably, the gene encoded by *tdh* assumes a pivotal function in the process of threonine degradation.[10,11] The elimination of this particular gene has been demonstrated to positively impact the augmentation of L-threonine. Another NAD-dependent threonine dehydrogenase encoded by the *yiaY* gene, along with knockdown of the *ltaE* gene encoding threonine aldolase, are also suggested to improve the L-threonine production,[12,13] whereas the *ilvA* and *tdcB* genes encoding threonine dehydratase play important roles in L-isoleucine production.[14,15] Numerous researchers have shown that in *E. coli*, a single knockdown of nonessential genes such as *yiaY*, *tdh*, and *ltaE* that are related to the threonine metabolic pathway contribute to the L-threonine production. As a result, we boldly chose to knock down these three genes simultaneously in the current study to fully understand their effects on the physiological properties of the bacterium itself.

To improve the production of L-isoleucine, we constructed a mutant strain with Δ*tdh*, Δ*ltaE* and Δ*yiaY* by knocking out genes related to threonine degradation using clustered regularly interspaced short palindromic repeats (CRISPR)/CRISPR-associated protein 9 (CRISPR/Cas9) gene editing technology. The mutant strain exhibited an augmentation in the synthesis of L-isoleucine, which was accompanied by a corresponding enhancement in the bacterial growth activity. We elucidated the effect of inactivation of the threonine metabolic pathway on the genetic characteristics of *E. coli* using transcriptomics, which further showed that the inactivated pathway had increased energy metabolism and a carbon flow bias toward L-isoleucine. We found that the mutant strain *E. coil* NXU102 L-isoleucine production was higher than the starting strain *E. coil* NXU101 (72.3%), while the biomass (OD_{600}) was higher than the starting strain (10.3%). These results suggested that attenuating the L-threonine metabolic

https://doi.org/10.1021/acsomega.3c07619
ACS Omega 2024, 9, 10276−10285

pathway could serve as one of the strategies to construct L-isoleucine high-yielding production strains.

MATERIALS AND METHODS

Strains, Plasmids, and Reagents. All strains, plasmids, and primers used in this study are listed in Tables 1 and 2. The recombinant *E. coli* NXU101 (Δ*LeuA*, Met^- + Lys^-) strain constructed previously in our laboratory was used as the starting strain,[16] while *E. coli* DH5α was used for cloning and plasmid construction. All bacterial strains were grown in an LB liquid medium or on an LB agar plate at 37 °C. The OPA derivatization reagent was prepared by dissolving 0.2014 g of OPA in 10 mL of methanol, and the solution was transferred to a 50 mL amber volumetric flask. Approximately 10 mL of β-mercaptoethanol was added to the flask, and the final volume was made up to 50 mL using methanol. For the preparation of pH 10.4 borate buffer, 6.19 g of boric acid and 6.52 g of KOH were dissolved in 200 mL of ultrapure water, and the solution pH was adjusted to 10.4 using metaphosphoric acid.

Table 1. Sources and Characteristics of Strains and Plasmids Used in This Study

strains	relevant characteristics	sources
E. coli K12 MG1655	wild type	laboratory collection[16]
E. coli NXU101	MG1655, Δ*leuA*/Met^- + Lys	laboratory collection[16]
E. coli NXU102	MG1655, Δ*leuA*/Met^- + Lys^-/Δ*tdh*/Δ*ltaE*/Δ*yiaY*	this study
plasmids		
pCas	repA101(Ts) kan Pcas-Red lacIqPtcr-sgRNA-pMB1	this study
pTargetF	pMB1 aadA sgRNA	this study
pTargetF-*tdh*	pMB1 aadA sgRNA-*tdh*	this study
pTargetF-*ltaE*	pMB1 aadA sgRNA-*ltaE*	this study
pTargetF-*yiaY*	pMB1 aadA sgRNA-*yiaY*	this study

Culture Medium and Culture Conditions. The strains were cultivated in LB medium, which consisted of 10 g of tryptone, 5 g of yeast extract, and 5 g of NaCl per liter. The pH of the medium was adjusted to 7.0 using 1 mol·L^{-1} NaOH. To solidify the medium, 1.5% (w/v) agar powder (Wako Pure Chemical Co., Ltd., Osaka, Japan) was added prior to autoclaving at 121 °C for 20 min. The defined medium for seed cultivation in the present study contained 5.0 g of glucose, 10.0 g of tryptone, 2.0 g of $(NH_4)_2SO_4$, 5.0 g of yeast powder, and 0.002 g of biotin per liter (Tianjin Damao Chemical Reagent Co. Ltd., Tianjin, China). The fermentation medium for L-isoleucine production contained 110.0 g of glucose, 21.0 g of corn pulp, 2.0 g of KH_2PO_4, 3.0 g of K_2HPO_4, 2 g of lysine, 20.5 g of $(NH_4)_2SO_4$, 0.01 g of $FeSO_4$ and 2.0 g of $MgSO_4$ per liter (Tianjin Damao Chemical Reagent Co. Ltd., Tianjin, China). The pH of both the seed and the fermentation media was adjusted to 7.0 using a 4.0 mol·L^{-1} NaOH solution.

The mutant strain NXU102 and the starting strain NXU101 were inoculated onto the LB solid medium and incubated overnight at 37 °C. Then, single colonies of each strain were picked from the LB solid medium, inoculated into seed medium, sealed with sterile gauze, and incubated at 37 °C for 12 h in a shaker at 200 rpm. Finally, the fermentation incubation was carried out under the same conditions for 40 h.

Genome Editing. Genetic deletion was performed by using the CRISPR/Cas9 system. The procedure has been described using *tdh* knockout as an example in this section. First, a gRNA expression plasmid (pTargetF-*tdh*) was constructed by using the pTargetF plasmid as a template and gRNA-*tdh*-S and gRNA-*tdh*-A as primers. Donor DNA fragments for the *tdh* deletion were prepared. Two pairs of

Table 2. Primers Used in This Experiment

primers	primer sequences (5′−3′)
gRNA-*tdh*-S	CTGGTGAAAAAGGCTCCAA
gRNA-*tdh*-A	CGTCATTGGGACCAACAGG
tdh-up-S	AGATAAAAGGGCTGGAATACCAGCCCTTGTTCGTGTTAATCCCAG
	CTCAGCATATGAATATCCTCCTTAGTTCCTATTC
tdh-down-A	GTAAACAACTGGGCGTTATCGCCTGAGGATGTGAGATGAAAGCG
	TTATCCGAGCTGCTTCGAAGTTCCTA
tdh-outF	CAGGTGAGAGAGTCACTTCAGGG
tdh-outR	CGGTTTCTTCTATCCGGTCGTTC
gRNA-*ltaE*-S	GTCAAGATGCGTCACCAGG
gRNA-*ltaE*-A	GACGTCTCGCGCGAACAAC
ItaE-up-S	GTTGCGGCACGTCTCTCTCCTTAACGCGCCAGGAATGCACGCCA
	GTGGGCGAGCTGCTTCGAAGTTCCTA
ItaE-down-A	AAGGGTGGCATTTCCCGTCATAATAAGGACATGCCATGATTGATT
	TACGCCATATGAATATCCTCCTTAGTTCCTATTC
ItaE-outF	GTTGCAGCTTTGCAAGCCTGTC
ItaE-outR	CATTCCACCGCAGATCAAACTCGAAC
gRNA-*tdh*-S	ATCGGGTTAGTAAAGCCAC
gRNA-*tdh*-A	GTGAAAGAAGAAGATTTCG
yiaY-up-S	GATAGTTGAAAAAGCGGCTAACAATTTGCCAGCCGTTGTGGAA
	ATGATGACATATGAATATCCTCCTTAGTTCCTATTC
yiaY-down-A	AAAATCCTCAGTAAGCTGCCCGCCCTTTTTTACACTTTCAGGAG
	TGTGTTGAGCTGCTTCGAAGTTCCTA
yiaY-outF	GTGTGAGGTATAACAAGGGTAGA
yiaY-outR	GATAATCAATAATACTGATCATATTTTCGAATG

https://doi.org/10.1021/acsomega.3c07619
ACS Omega 2024, 9, 10276−10285

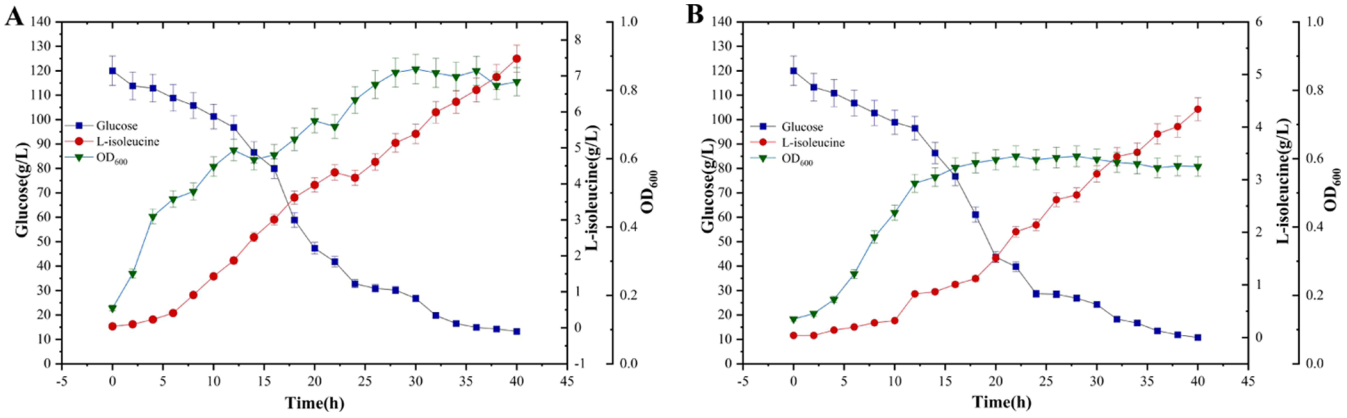

Figure 2. Comparison of batch fermentation results of the mutant strain NXU102 (A) and the starting strain *E. coli* NXU101 (B). Error bars represent standard deviations from three parallel replicates.

primers, *tdh*-up-S and *tdh*-down-A, were used to amplify upstream homologue arm M1 and downstream homologue arm M2. Second, M1 and M2 were ligated via overlapping extension PCR, generating a donor DNA fragment (DNA-*tdh*). Third, pTargetF-*tdh* and DNA-*tdh* were cotransformed into *E. coli* NXBG-11−3 competent cells containing a pCas plasmid via electrotransformation. The incubated bacterial suspension was spread on LB plates with kanamycin and chloramphenicol to confirm the presence of the pTargetF-*tdh* and pCas plasmids. Positive colonies were validated using colony PCR, and mutations were confirmed through DNA sequencing. Then, positive colonies verified by PCR were inoculated in LB medium containing kanamycin and IPTG and cultured overnight at 42 °C to destroy the temperature-sensitive pCas plasmid of the mutant. The appropriate *tdh* knockout strain was obtained by PCR verification. Finally, the appropriate *tdh* knockout strain was obtained by PCR verification.

Analytical Methods. Cell density was monitored by measuring the absorbance at 600 nm by using a V-5100 ultraviolet spectrophotometer (Metash, Shanghai, China). The concentration of residual glucose in the fermentation medium was detected by using a biosensor analyzer (SBA-40E, Shandong, China). The content of L-isoleucine in the fermentation medium was measured using high-performance liquid chromatography (HPLC) (UFLC0303062304, Shimadzu, Japan) on an Agilent C18 column (4.6 mm × 250 mm, 5 μm, Agilent, Shanghai, China) at 30 °C, with mobile phase consisting of acetonitrile/water at a flow rate of 1.0 mL·min^{-1}. Approximately 20 μL of fermentation broth supernatant was measured, and 20 μL of an internal reference solution (ultrapure water or 10 μmol·L−1 L-isoleucine standard solution) was added to the broth supernatant, followed by 10 μL of the OPA derivatization reagent after thorough mixing. The derivatization reaction was carried out for 2 min and was immediately diluted to 100 μL with a 1:9 mixture of anhydrous ethanol and borate buffer solution. An HPLC injection volume for all samples was 20 μL. All data were expressed as the mean ± standard deviation of three replicates.

Whole-Genome Transcriptional Analysis. The starting strain *E. coli* NXU101 and the mutant strain NXU102 were inoculated in LB liquid medium, and the precipitates of the log phase (OD_{600} value of 0.8−1.0) were collected, snap-frozen in liquid nitrogen, and stored at −80 °C.

Total RNA was extracted from *E. coli* NXU101 and the mutant strain using TRNzol Universal Reagent (DP424, Tiangen Biotech (Beijing) Co., Ltd.) according to the manufacturer's instructions. The concentration and purity of RNA were detected using a Nano Drop 2000 microspectrophotometer, RNA integrity was detected through agarose gel electrophoresis, and RQN values were analyzed with an Agilent 5300 Fragment Analyzer (Agilent, Technologies, CA). The RNA samples were sent to Majorbio (Shanghai, China) for transcriptome sequencing using the Illumina HiSeq-4000 sequencing platform. The genome of *E. coli* K-12 MG1655 (NC_000913.3) was used as the reference genome to assemble and analyze the RNA-seq data. Differentially expressed genes (DEGs) were functionally annotated by using the public Kyoto Encyclopedia of Genes and Genomes (KEGG) and gene ontology (GO) databases.

The expression levels of genes and transcripts were quantified using the quantitative software RSEM with TPM. After obtaining read counts of the genes, DESeq2, DEGseq, and edgeR were used to analyze the differential expression of genes between samples and between groups. Genes, in which the *P*-value and FDR (*q*-value) were lesser than 0.05 and the amount of change in expression was greater than 2-fold, were identified as significantly differentially expressed (PRJNA990347).

RESULTS

Construction of the Mutant Strain NXU102. The results of the *tdh*, *ltaE*, and *yiaY* gene knockout by CRISPR gene-editing technology are shown in Figures S1−S3. The length of the starting strain amplification products was found to be 1567, 1106, and 1567 bp, respectively, when PCR was performed with primer pairs on the outer side of the genome homologous arms. The length of the amplification products for these primers was reduced to 405, 416, and 306 bp when the *tdh*, *ltaE*, and *yiaY* genes were knockout, respectively.

Mutant Strain NXU102 Shake Flask Fermentation Culture. The biomass and glucose consumption by the starting strain *E. coli* NXU101 and the mutant strain NXU102 were measured, and the results are displayed in Figure S1. The growth trends of the mutant strain and the starting strain were basically the same for the first 10 h. After 10 h, the two strains demonstrated different growth states, where the mutant strain NX102 continued to accumulate, while the starting strain NX101 began to stabilize. Surprisingly, sugar consumption of the mutant strain did not change significantly compared to the starting strain *E. coli* NXU101. Overall, the resulting mutant

https://doi.org/10.1021/acsomega.3c07619
ACS Omega 2024, 9, 10276−10285

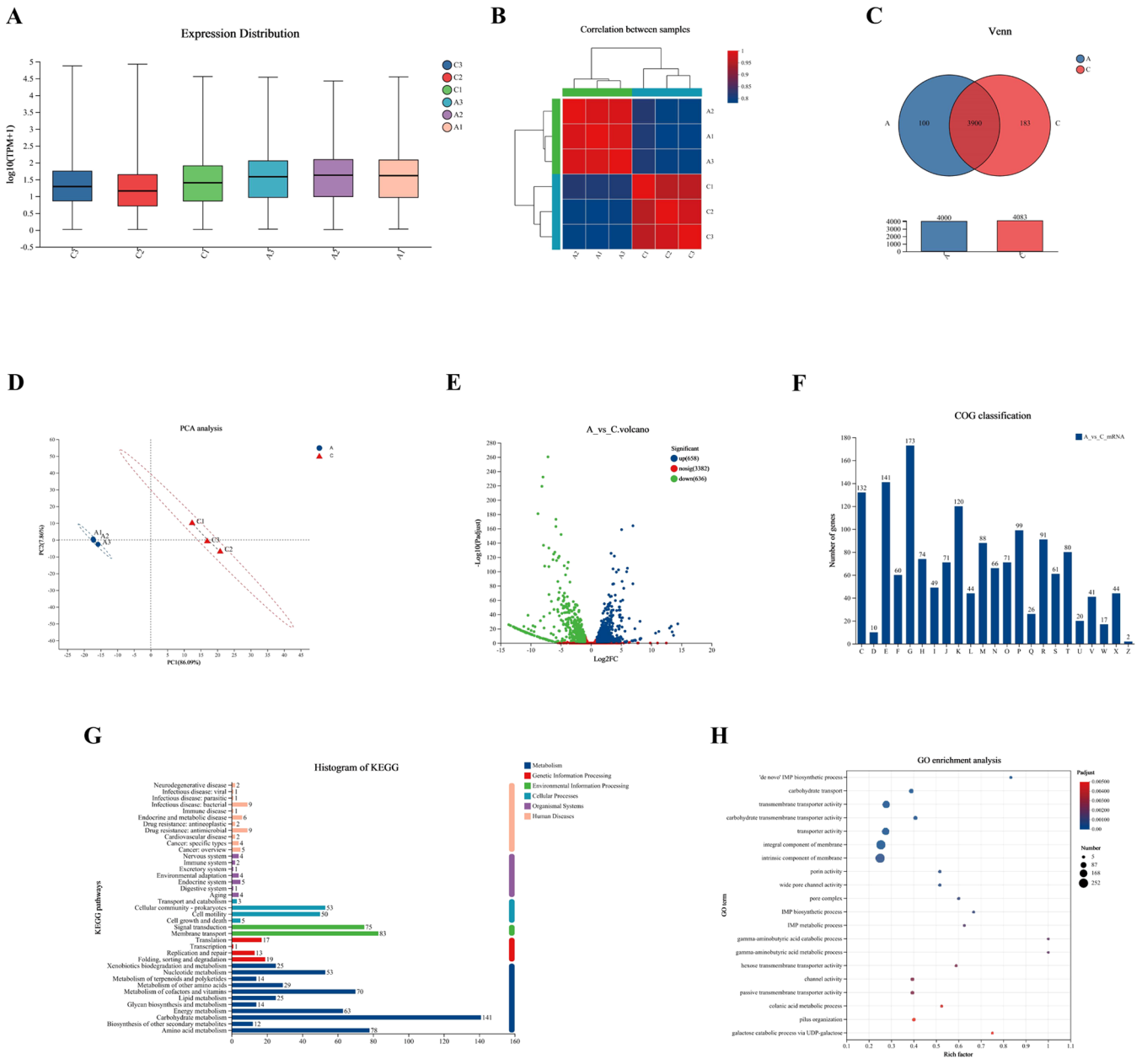

Figure 3. Alterations of *E. coli* gene expression induced by inactivation of the threonine metabolic pathway, where A is *E. coli* NXU101 and C is the mutant strain *E. coli* NXU102. (A) Boxplot indicated the gene expression distribution of each sample. (B) Plot indicated a correlation between biological repetitions. (C) Análisis del diagrama de Ven de los genes expresados diferencialmente (D) PCA (principal component analyses) of the mutant strain NXU102 gene expression profiles. PC1, principal component 1; PC2, principal component 2. Explained variants PC1:86.09% and PC2:7.86%. (E) Volcano plot of the up- and down-regulated genes by the mutant strain NXU102. (F) COGs (clusters of orthologous groups) function classification figure; C: energy production and conversion; D: cell cycle control, cell division, chromosome partitioning; E: amino acid transport and metabolism; F: nucleotide transport and metabolism; G: carbohydrate transport and metabolism; H: coenzyme transport and metabolism; I: lipid transport and metabolism; J: translation, ribosomal structure, and biogenesis; K: transcription; L: replication, recombination, and repair; M: cell wall/membrane/envelope biogenesis; N: cell motility; O: posttranslational modification, protein turnover, chaperones; P: inorganic ion transport and metabolism; Q: secondary metabolites biosynthesis, transport, and catabolism; R: general function prediction only; S: function unknown; T: signal transduction mechanisms; U: intracellular trafficking, secretion, and vesicular transport; V: defense mechanisms; W: extracellular structures; X: mobilome; and Z: cytoskeleton. (G) KEGG categories indicated significantly enriched functions for DEGs: the starting strain *E. coli* NXU101 vs the mutant strain NXU102. Genes were divided into six branches according to the biological pathways they participated in metabolism, genetic information processing, environmental information processing, cellular processes, organismal systems, and human diseases. (H) Top-ranked GO (gene ontology) terms of the DEGs (differentially expressed genes): the starting strain *E. coli* NXU101 vs the mutant strain NXU102. The size of each bubble reflects the number of DEGs assigned to the GO terms.

strain NXU102 exhibited the highest final glucose consumption of 106.7 ± 0.2 g·L^{-1} and a maximum cell density of 0.862 ± 0.008 at OD_{600} (the OD value was reduced by a factor of 10 to better represent the data in this study). On the other hand, the resulting starting strain *E. coli* NXU101 exhibited the highest final glucose consumption of 110.2 ± 0.2 g·L^{-1} and a maximum cell density of 0.781 ± 0.008 at OD_{600}. Both the *E. coli* NXU101 starting strain and the NXU102

https://doi.org/10.1021/acsomega.3c07619
ACS Omega 2024, 9, 10276−10285

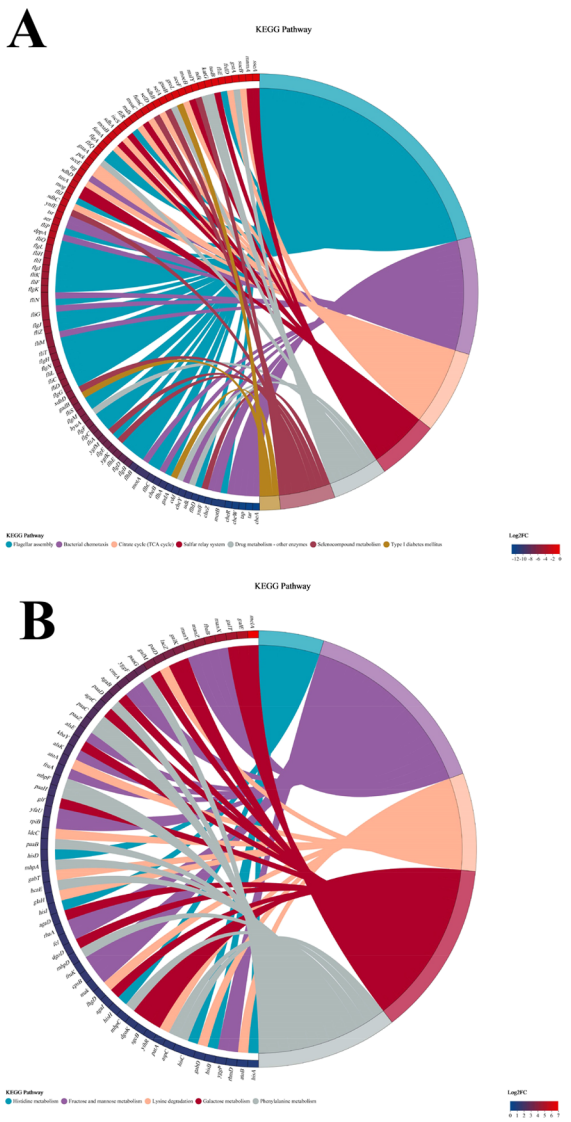

C

Gene name	Description	Log2fc
patD	Gamma-aminobutyraldehyde dehydrogenase	3.454085
gabD	Succinate-semialdehyde dehydrogenase (NADP(+)) GabD	1.238749
lhgD	L-2-hydroxyglutarate dehydrogenase	1.421682
gabT	4-aminobutyrate aminotransferase GabT	1.655234
ldcC	lysine decarboxylase 2	1.752535
patA	putrescine aminotransferase	1.287674
atoB	acetyl-CoA acetyltransferase	1.082387
glaH	glutarate dioxygenase GlaH	1.572392
atoA	acetyl-CoA:acetoacetyl-CoA transferase subunit beta	2.071876

D

Gene name	Description	log2fc
sdhD	succinate:quinone oxidoreductase%2C membrane protein SdhD	-2.518
sdhC	succinate:quinone oxidoreductase%2C membrane protein SdhC	-2.721
pck	phosphoenolpyruvate carboxykinase (ATP)	-2.109
aceE	pyruvate dehydrogenase E1 component	-2.295

E

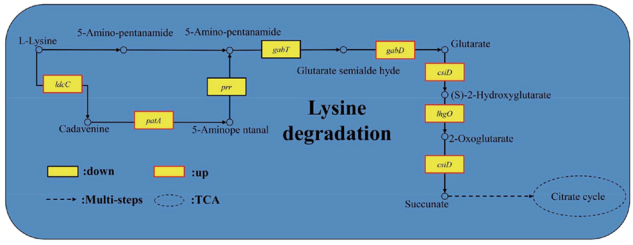

Figure 4. Detailed analysis of the enriched KEGG pathway involved L-isoleucine production and gene sets. (A) Circos plots with interdependence between selected KEGG pathways and their up-regulated genes. (B) Circos plots with interdependence between selected KEGG pathways and their down-regulated genes. (C) Up-regulated genes in genes related to lysine degradation and description. (D) Genes associated with the TCA cycle in down-regulated genes and description. (E) Expression of lysine degradation-related genes in the pathway.

mutant strain were fermented simultaneously, and the supernatant samples were centrifuged for the determination of L-isoleucine yields. Interestingly, the amount of L-isoleucine produced by *E. coli* NXU101 was 4.34 ± 0.08 g·L^{-1} while the mutant strain NXU102 was 72.3% higher than the starting strain at 7.48 ± 0.01 g·L^{-1} after 40 h of fermentation (Figure 2).

Transcriptional Analysis of *E. coli* NXU101 and *E. coli* NXU102. Transcriptome sequencing was performed on the starting strain *E. coli* NXU101 and the mutant strain NXU102 from distinct groups in this study. Subsequently, the expression matrices were assembled based on the original sequencing outcomes, where the expression matrix of the mutant strain NXU102 was investigated and analyzed. The reliability of the subsequent differentially expressed genes (DEGs) was confirmed through the examination of expression distribution (Figure 3A), sample correlation (Figure 3B), and PCA analysis (Figure 3D). Venn analysis among the samples revealed that there were 100 specifically expressed genes in group A and 183 specifically expressed genes in group C. The volcano map of differential expression showed up to 1294 DEGs between the starting strain *E. coli* NXU101 and the mutant strain NXU102 (Figure 3E). Among them, a total of 658 genes were up-regulated, and 636 were down-regulated. The DEGs identified in this study underwent further bioinformatics analysis to determine their functional characteristics. This analysis included COG classification, GOG enrichment analysis, and histogram of KEGG. The COG classification results indicated that 152 genes/transcripts within this gene set that correspond to 9.6% of the total DEGs were classified as poorly characterized. Despite this, 47.6% of the DEGs were classified as metabolism category that was involved in the metabolic pathways (Figure 3G), including 173 DEGs, which were annotated to "carbohydrate transport and metabolism," 132 DEGs, which were annotated to "energy production and conversion," and 141 DEGs, which were annotated to "amino acid transport and metabolism" (Figure 3F). Figure 3H shows the GO analysis that revealed the top 20 most enriched GO

https://doi.org/10.1021/acsomega.3c07619
ACS Omega 2024, 9, 10276−10285

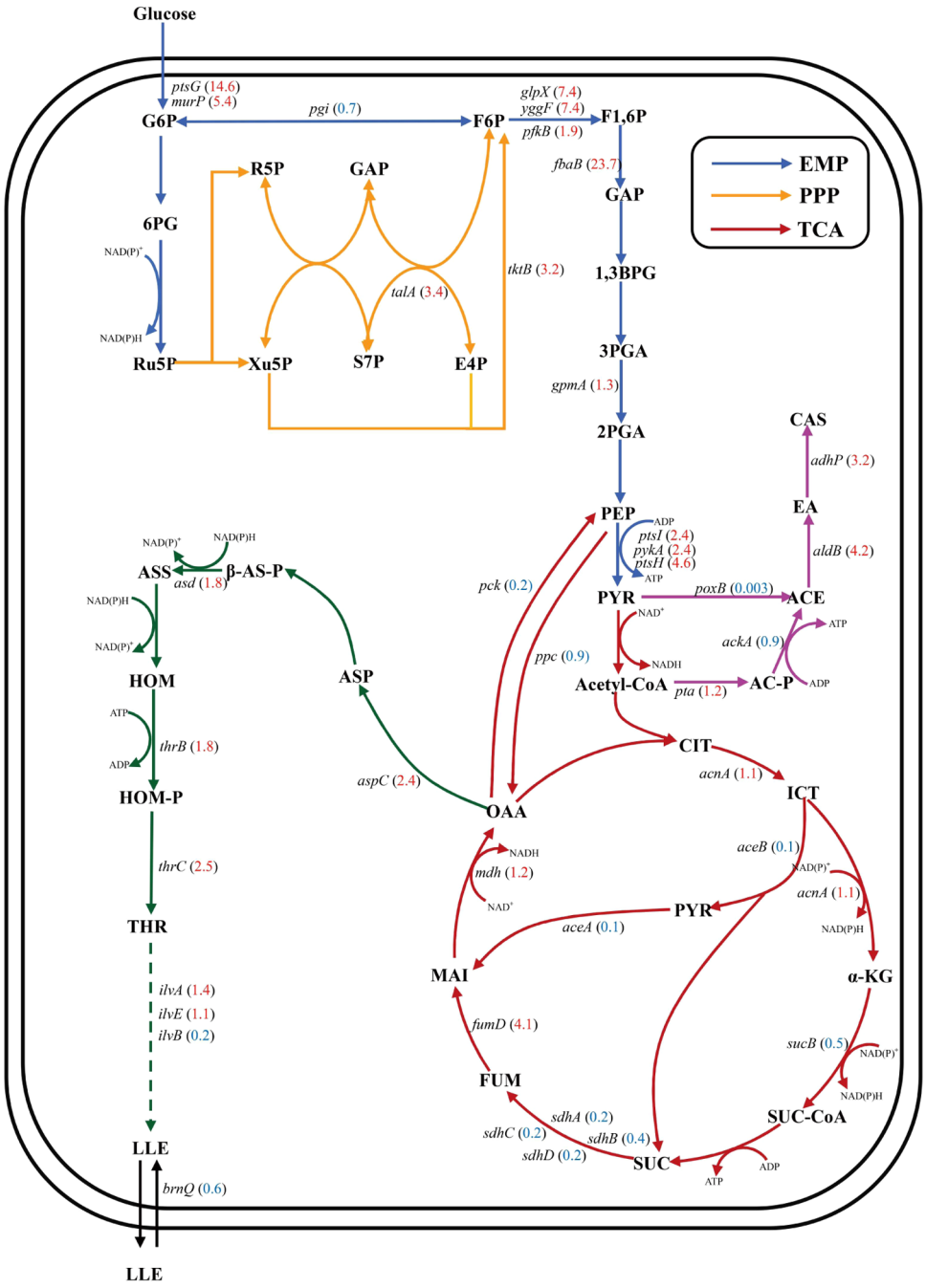

Figure 5. Transcriptional differences in related genes between the departure strain NXU101 and the mutant strain NXU102. The number in parentheses is the ratio of the average value of the mRNA fragments of a gene in *E. coli* NXU102 to that in *E. coli* NXU101. Red indicates a significant increase in transcription, and green indicates a significant decrease in transcription.

terms on the basis of the *P*-value ($P = 0$), where reductase activity, acting on CH or CH_2 groups, and NAD or NADP as acceptor were found to be the important pathway.

The heat map in Figure 4A shows 3 metabolic pathways of amino acids including histidine metabolism, lysine degradation, and phenylalanine metabolism. Figure 4C shows that 9 DEGs belong to the lysine degradation, including *patD*, *gabD*, *lhgD*, *gabT*, *ldcC*, *patA*, *atoB*, *glaH*, and *atoA*. The pathways in Figure 4B,D show that 4 DEGs belong to the TCA cycle, including *sdhD*, *sdhC*, *pck*, and *aceE*. Figure 4C,D shows the difference of related pathways for the DEGs according to their log2 fold change values (Log2 fc). The most relevant lysine catabolic pathway was analyzed, and a significant amount of genes in the lysine to succinate pathway were up-regulated, which might lead to high carbon flow to the TCA cycle.

Genes related to L-isoleucine metabolism showing KEGG enrichment were further analyzed in the present study (Figure 5). The transcription levels of *ptsG* and *murP* genes participating in PTS were significantly up-regulated. Among the genes associated with the glycolytic pathway (EMP), *glpX*, *yggF*, *pfk*, *fbaB*, *gpmA*, *ptsGH*, and *pykA* were significantly up-regulated, while *pgi* was significantly down-regulated. The transcription levels of *aceAB*, *sdhABCD*, and *sucB* genes that were involved in the TCA cycle were significantly down-regulated, while *mdh*, *acnA*, and *fumD* were significantly up-regulated. Interestingly, phosphoenolpyruvate to oxaloacetate-

https://doi.org/10.1021/acsomega.3c07619
ACS Omega 2024, 9, 10276−10285

related genes, such as *ppc* and *pck*, were down-regulated by 0.9- and 0.2-fold, respectively. In comparison, *ppc* (the gene encoding phosphoenolpyruvate carboxylase) might be more strongly expressed, which was useful to improve the yield of the target product in this study. In the group of the genes participating in the L-isoleucine synthesis pathway, *aspC*, *asd*, *thrBC*, and *ilvAE* showed significant up-regulated transcription levels, while *ilvB* exhibited down-regulated transcription levels. One of them, *ilvA*, encoded a threonine dehydratase, which is the key enzyme for the production of L-isoleucine from L-threonine after the 5-step reaction. Similarly, a 2.4-fold upregulation of *aspC* (the gene encoding aspartate aminotransferase) also greatly increased carbon flow to the aspartate pathway. It was unexpected to observe the *poxB* gene to be down-regulated by 0.003-fold for encoding the pyruvate dehydrogenase, while *the adhP* and *aldB* genes were significantly up-regulated, which would lead to a redistribution of the carbon flow. The *pta* gene, which is related to acetyl coenzyme degradation, was found to be up-regulated by 1.2-fold, while the *ackA* gene, which is related to the ATP production in this pathway, was down-regulated by 0.9-fold. Nevertheless, such changes might not have a significant impact on the overall ATP supply compared with the down-regulation of other genes. Although a large number of genes in the TCA cycle were down-regulated, a great amount of genes participating in the EMP and oxidative phosphorylation pathways were also found to be up-regulated. In particular, the upregulation of genes related to NADPH and ATP production might be responsible for the enhanced activity of the mutant strains. A reduced accumulation of the byproduct acetic acid in the biosynthetic pathway had lowered its detrimental effect on the bacterium and was thus beneficial to the normal growth of the bacterium. At the same time, by cutting off the degradation pathway of L-threonine, the accumulation of L-threonine was enhanced and the carbon flow was redirected to the L-isoleucine metabolic pathway.

DISCUSSION

L-isoleucine is widely used in the food industry, biomedicine, and cosmetics with high added value. Therefore, it is urgent to construct a chassis strain with a high production of L-isoleucine, which is an important precursor of L-isoleucine, and we aim to increase the accumulation of L-isoleucine by cutting off its metabolic pathway. We analyzed the transcriptome of the strain to further understand its physiological properties and to provide ideas for the construction of L-isoleucine chassis strains.

L-isoleucine is mainly produced by microbial fermentation, with *E. coli* and *C. glutamicum* being the main production strains.[2,17] *E. coli* usually synthesizes high levels of acetate, which may affect the production of L-isoleucine by inhibiting cell growth and protein production.[18] However, the biosynthesis of L-isoleucine in *E. coli* can be improved by optimizing the fermentation process or by knocking out genes related to acetate production. Although the yield of current shake flask fermentation using *E. coli* at 12 g·L^{-1} is lower than the yield of L-isoleucine in *C. glutamicum* at 32 g·L^{-1},[19] the *E. coli* genome is more well-characterized compared with *C. glutamicum*. Further, several tools have been developed for the cytogenetic manipulation of *E. coli*.[20]

In this study, genes related to the L-threonine degradation (Δ*tdh*, Δ*ltaE*, Δ*yiaY*) were knocked out using CRISPR/Cas9 gene editing technology to obtain the *E. coli* NXU102 mutant strain. The yield of L-isoleucine in this mutant strain was found to be 7.48 g·L^{-1}, demonstrating good genetic stability and stable L-isoleucine production. At the same time, it is important to fully understand the effect of genetic changes in the mutant strain on the L-isoleucine synthesis pathway through transcriptomics. An analysis of DEG transcript levels in the relevant pathways could also provide a deeper mechanistic insight into further strain modification.

Transcriptional analysis of the mutant strain NXU101 showed that DEGs were mainly enriched in the L-isoleucine synthesis pathways, such as oxidative phosphorylation, TCA cycle, phosphotransferase system, and amino acid metabolism. The EMP pathway, the PPP pathway, and the TCA cycle generate precursors and energy required for the synthesis of L-isoleucine.[21,22] In the mutant strain NXU101, *ptsG* and *murP* gene expressions were up-regulated, implying that more glucose had entered the *E. coli* cells through the phosphotransferase system.[23] It is important to highlight again that the EMP pathway, the PPP pathway, and the TCA cycle are key pathways for the synthesis of the L-isoleucine precursor, such as oxaloacetate, aspartate, and NADPH,[24] and the TCA cycle is a major pathway in microbial oxidative metabolism. The *sdhABCD* genes encode four subunits of succinate dehydrogenase, whose expression was found to be down-regulated in the mutant strain NXU101 in this study.[25] This might lead to a blockage of succinate in the TCA cycle.[26] Interestingly, the *fumD* and *mdh* genes were significantly up-regulated and were able to direct the carbon flow toward oxaloacetate to enhance the production of bulk biochemicals. On the other hand, the EMP pathway is a fundamental biochemical infrastructure of carbohydrate metabolism in *E. coli*, providing ATP for cell growth and metabolism whereby cells are able to produce ATP through phosphorylation of the EMP pathway substrates. Studies have shown that hypoxia may lead to the upregulation of EMP pathway genes, and the EMP pathway can still provide energy to support microbial growth when the TCA cycle is inhibited. In this study, an increased transcript level of the key EMP pathway genes (e.g., *glpX*, *yggF*, *pfk*, *fbaB*, *gpmA*, *ptsGH*, and *pykA*) was found to be able to maintain normal microbial growth.

In *E. coli*, the detrimental effects of high levels of acetate are limiting the bacteria's growth. Simen Akkermans et al. investigated the effect of pH on the growth of *E. coli* K12 MG1655 using a γ-interaction model and showed that the growth rate and maximum cell density increased as the pH reached 7.0.[27] In this study, the *poxB* gene was significantly down-regulated in the mutant strain NXU101, which might be responsible for the enhanced growth activity and increased production of L-isoleucine in *E. coli*. By overexpressing the *yggE* gene, Yoshihiro Ojima et al. found that the expression levels of the acetic acid production gene (e.g., *pta*, *ackA*, and *poxB*) were relatively low, especially the expression level of *poxB* that was one-seventh of the original strain, and the acetic acid yield in culture fermentation was only half of the original strain.[28] Meanwhile, the transcript levels of the *aldB* and *adh* genes were significantly up-regulated, probably due to the reduction of acetic acid production/accumulation.

Phosphoenolpyruvate carboxylase (encoded by the *ppc* gene) and phosphoenolpyruvate carboxykinase (encoded by the *pck* gene) were both down-regulated in *E. coli* under glycolytic conditions. The known functions of the *pck* gene are the decarboxylation of oxaloacetate under gluconeogenic conditions and ATP exclusion for the metabolic balance of

https://doi.org/10.1021/acsomega.3c07619
ACS Omega 2024, 9, 10276−10285

cells.[29] This might be due to the up-regulation of a large number of genes in the EMP pathway of the mutant strain, which resulted in a reduction in the *pck* gene expression. By constructing *E. coli* that expressed natural *pck* and *ppc* genes under the same promoter control, studies found that the natural *pck* gene activity was 160-fold lower than the *ppc* gene,[30] which explained the higher expression of the *ppc* gene compared with the *pck* gene in the mutant strain. Peng et al. constructed a *ppc* mutant and found reduced acetate and CO_2 excretion in the mutant using metabolic flux analysis C13 labeling experiments, while TCA cycle-related genes were up-regulated and glycolytic together with pentose phosphate pathways were down-regulated. The concentrations of acetyl coenzyme A and oxaloacetate were also decreased in the *ppc* mutant.[31] Similar to Peng et al., *ppc* gene expression in the mutant strains was also down-regulated in this study, which is in surprising agreement with his contrary description. Meanwhile, NAD (+)-dependent malate dehydrogenase as encoded by the *mdh* gene is an energy supply enzyme that catalyzes the interconversion of malate and oxaloacetate and plays a key role in several metabolic pathways including the TCA cycle.

The *ilvA* gene that encodes threonine deaminase was significantly up-regulated in the present study, and the enzyme was resistant to feedback inhibition by L-isoleucine. By introducing the *ilvA* gene into wild Bacillus flavus, Hashiguchi et al. constructed a mutant strain capable of converting exogenous L-homoserine and L-threonine to L-isoleucine, and the transformants had obtained a high accumulation of L-isoleucine.[32] Guillouet et al. found that overexpression of the *ilvA* gene in *C. glutamicum* was able to increase the yield of L-isoleucine by 50-fold, whereas overexpression of the *tdcB* gene increased the target product by only 4-fold. It was also noticed that 70% of the carbon available in the lysine pathway was redirected to L-isoleucine when the *ilvA* gene was overexpressed.[14] This is consistent with the current finding that observed the upregulation of the *ilvA* gene was accompanied by significant upregulation of the L-lysine degradation pathway-related genes, such as *patD*, *gabD*, *lhgD*, *gabT*, *ldcC*, *patA*, *atoB*, *glaH*, and *atoA*, allowing the degradation of lysine to succinate that re-entered the TCA cycle.

E. coli NXU101 (Δ*LeuA*, Met-+Lys-) with an L-isoleucine yield of 4.34 $g{\cdot}L^{-1}$ served as the starting strain in this study. The mutant strain NXU102 was successfully constructed by cutting off the L-threonine catabolic pathway through the CRISPR/Cas9 gene editing technology. The yield of L-isoleucine was 7.48 $g{\cdot}L^{-1}$, which was 72.3% higher than the starting strain *E. coli* NXU101, and the activity was found to be 10.3% higher than the starting strain. In order to fully understand the altered genetic characteristics of the mutant strains and to prepare for further genetic modification, transcriptome analysis of the starting and mutant strains was conducted. The results of the transcriptome analysis indicated that genes related to the EMP pathway were up-regulated, which facilitated energy production and strain activity. On the other hand, genes related to the detrimental byproduct acetate degradation pathway were up-regulated, but the production genes were down-regulated, which is beneficial for energy production as well as the activity of the strain theoretically. Similarly, the *poxB* gene was down-regulated to 0.003-fold, which reduced the byproduct production, whereas the *aspC* gene up-regulated to 2.4-fold, which promoted the flow of oxaloacetate to L-aspartate and facilitated the synthesis of L-isoleucine precursors. Up-regulation of the *ilvA* gene by 1.4 enhanced L-threonine metabolism to produce L-isoleucine. Therefore, the mutant strain NXU102 showed a significant increase in its activity and L-isoleucine production, which provides insights for the construction of an L-isoleucine-producing engineered strain of *E. coli*, whereby a high-quality chassis strain can be harvested.

■ ASSOCIATED CONTENT

Data Availability Statement

All the data supporting the findings of this study are available within the article and its Supporting Information files. Data is available on request from the authors. The data that support the findings of this study are available from the corresponding author, [H.T.F], upon reasonable request.

Supporting Information

The Supporting Information is available free of charge at https://pubs.acs.org/doi/10.1021/acsomega.3c07619.

Knockout results of this experiment (PDF)

■ AUTHOR INFORMATION

Corresponding Author

Haitian Fang − *Ningxia Key Laboratory for Food Microbial-Applications Technology and Safety Control, School of Food Science and Engineering, Ningxia University, Yinchuan 750021, China*; Email: fanght@nxu.edu.cn

Authors

HaoJie Zhang − *Ningxia Key Laboratory for Food Microbial-Applications Technology and Safety Control, School of Food Science and Engineering, Ningxia University, Yinchuan 750021, China*; orcid.org/0000-0002-7123-1637

Tong Ye − *Ningxia Key Laboratory for Food Microbial-Applications Technology and Safety Control, School of Food Science and Engineering, Ningxia University, Yinchuan 750021, China*

Liu Fengmin − *Ningxia Key Laboratory for Food Microbial-Applications Technology and Safety Control, School of Food Science and Engineering, Ningxia University, Yinchuan 750021, China*

Xiangjun Zhang − *School of Life Science, Ningxia University, Yinchuan 750021, China; Ningxia Key Laboratory for Food Microbial-Applications Technology and Safety Control, School of Food Science and Engineering, Ningxia University, Yinchuan 750021, China*

Jipeng Wang − *Ningxia Key Laboratory for Food Microbial-Applications Technology and Safety Control, School of Food Science and Engineering, Ningxia University, Yinchuan 750021, China*

Xiaobo Wei − *Ningxia Key Laboratory for Food Microbial-Applications Technology and Safety Control, School of Food Science and Engineering, Ningxia University, Yinchuan 750021, China*

Yun Ping Neo − *School of Biosciences, Faculty of Health and Medical Sciences, Taylor's University, Subang Jaya, Selangor 47500, Malaysia*

Huiyan Liu − *Ningxia Key Laboratory for Food Microbial-Applications Technology and Safety Control, School of Food Science and Engineering, Ningxia University, Yinchuan 750021, China*

Complete contact information is available at: https://pubs.acs.org/10.1021/acsomega.3c07619

https://doi.org/10.1021/acsomega.3c07619
ACS Omega 2024, 9, 10276−10285

Author Contributions

Conceptualization, H.J.Z., H.T.F., and H.Y.L.; methodology, H.T.F.; H.J.Z., and F.-M. L.; software, H.J.Z., T.Y., and C.M.; formal analysis, H.Y.L. and H.T.F.; original draft preparation, H.J.Z.; review and editing, H.T.F., X.B.W., and Y.P.N; supervision and administration, H.T.F and H.Y.L; and funding acquisition, H.T.F. and H.Y.L. All authors have read and agreed to the published version of the manuscript.

Funding

This research was supported by the Natural Science Foundation of Ningxia (2020AAC03100); the Innovation Platform Funds of Ningxia Key Laboratory for Food Microbial-Applications Technology and Safety Control (2021DPC05003); and the Youth Science and Technology Innovation Personnel Training Project of Ningxia.

Notes

The authors declare no competing financial interest.

REFERENCES

(1) Gu, C. S.; Mao, X. B.; Chen, D. W.; Yu, B.; Yang, Q. Isoleucine Plays an Important Role for Maintaining Immune Function. *Curr. Protein Pept. Sci.* **2019**, *20*, 644−651.

(2) Becker, J.; Giesselmann, G.; Hoffmann, S. L.; Wittmann, C. In *Corynebacterium glutamicum for Sustainable Bioproduction: From Metabolic Physiology to Systems Metabolic Engineering*; Zhao, H.; Zeng, A. P. 2018; Vol. *162*.

(3) Li, Y.; Wei, H.; Wang, T.; Xu, Q.; Zhang, C.; Fan, X.; Ma, Q.; Chen, N.; Xie, X. Current status on metabolic engineering for the production of L-aspartate family amino acids and derivatives. *Bioresour. Technol.* **2017**, *245*, 1588−1602.

(4) Lu, S.; Tao, T.; Su, Y. T.; Hu, J.; Zhang, L.; Wang, G. L.; Li, X. Y.; Guo, X. H. Whole Genome Sequencing and CRISPR/Cas9 Gene Editing of Enterotoxigenic *Escherichia coli* BE311 for Fluorescence Labeling and Enterotoxin Analyses. *Int. J. Mol. Sci.* **2022**, *23*, No. 7502.

(5) Korthikunta, V.; Pandey, J.; Singh, R.; Srivastava, R.; Srivastava, A. K.; Tamrakar, A. K.; Tadigoppula, N. In vitro anti-hyperglycemic activity of 4-hydroxyisoleucine derivatives. *Phytomedicine* **2015**, *22*, 66−70.

(6) Zhang, C. L.; Ma, J.; Li, Z. X.; Liang, Y. L.; Xu, Q. Y.; Xie, X. X.; Chen, N. A strategy for L-isoleucine dioxygenase screening and 4-hydroxyisoleucine production by resting cells. *Bioengineered* **2018**, *9*, 72−79.

(7) D'Este, M.; Alvarado-Morales, M.; Angelidaki, I. Amino acids production focusing on fermentation technologies - A review. *Biotechnol. Adv.* **2018**, *36*, 14−25.

(8) Dong, X. Y.; Zhao, Y.; Zhao, J. X.; Wang, X. Y. Characterization of aspartate kinase and homoserine dehydrogenase from *Corynebacterium glutamicum* IWJ001 and systematic investigation of L-isoleucine biosynthesis. *J. Ind. Microbiol. Biotechnol.* **2016**, *43*, 873−885.

(9) Yamamoto, K.; Tsuchisaka, A.; Yukawa, H. In *Branched-Chain Amino Acids*. Adv Biochem Eng Biotechnol, 2017, 10; Vol. *159*.

(10) Yu, H.; Xu, J.; Liu, L.; Zhang, W. [Biosynthesis of 2,5-dimethylpyrazine from L-threonine by whole-cell biocatalyst of recombinant *Escherichia coli*]. *Sheng Wu Gong Cheng Xue Bao = Chinese Journal of Biotechnology* **2021**, *37*, 228−241.

(11) Lee, K. H.; Park, J. H.; Kim, T. Y.; Kim, H. U.; Lee, S. Y. Systems metabolic engineering of *Escherichia coli* for L-threonine production. *Mol. Syst. Biol.* 2007, *3*.

(12) Vybornaya, T. V.; Yuzbashev, T. V.; Fedorov, A. S.; Bubnov, D. M.; Filippova, S. S.; Bondarenko, F. V.; Sineoky, S. P. Use of an Alternative Pathway for Isoleucine Synthesis in Threonine-Producing Strains of *Escherichia coli*. *Appl. Biochem. Microbiol.* **2020**, *56*, 759−769.

(13) Liu, J. Q.; Dairi, T.; Itoh, N.; Kataoka, M.; Shimizu, S.; Yamada, H. Gene cloning, biochemical characterization and physiological role of a thermostable low-specificity L-threonine aldolase from *Escherichia coli*. *Eur. J. Biochem.* **1998**, *255*, 220−226.

(14) Guillouet, S.; Rodal, A. A.; An, G. H.; Lessard, P. A.; Sinskey, A. J. Expression of the *Escherichia coli* catabolic threonine dehydratase in *Corynebacterium glutamicum* and its effect on isoleucine production. *Appl. Environ. Microbiol.* **1999**, *65*, 3100−3107.

(15) Chen, L.; Chen, Z.; Zheng, P.; Sun, J. B.; Zeng, A. P. Study and reengineering of the binding sites and allosteric regulation of biosynthetic threonine deaminase by isoleucine and valine in *Escherichia coli*. *Appl. Microbiol. Biotechnol.* **2013**, *97*, 2939−2949.

(16) Zhiyu Ai Thesis, 2022.

(17) Park, J. H.; Lee, S. Y. Metabolic pathways and fermentative production of L-aspartate family amino acids. *Biotechnol. J.* **2010**, *5*, 560−577.

(18) DAGLEY, S.; DAWES, E. A.; FOSTER, S. M. Effect of pH on growth of Aerobacter aerogens and *Escherichia coli* in synthetic media. *Biochem. J.* **1952**, *52*, xxi−xxii.

(19) Wang, X. Strategy for improving L-isoleucine production efficiency in *Corynebacterium glutamicum*. *Appl. Microbiol. Biotechnol.* **2019**, *103*, 2101−2111.

(20) Chang, Y.; Su, T.; Qi, Q.; Liang, Q. Easy regulation of metabolic flux in *Escherichia coli* using an endogenous type I-E CRISPR-Cas system. *Microb. Cell. Fact.* **2016**, *15*, 195.

(21) Seol, E.; Sekar, B. S.; Raj, S. M.; Park, S. Co-production of hydrogen and ethanol from glucose by modification of glycolytic pathways in *Escherichia coli*- from Embden-Meyerhof-Parnas pathway to pentose phosphate pathway. *Biotechnol. J.* **2016**, *11*, 249−256.

(22) Murarka, A.; Clomburg, J. M.; Moran, S.; Shanks, J. V.; Gonzalez, R. Metabolic Analysis of Wild-type *Escherichia coli* and a Pyruvate Dehydrogenase Complex (PDHC)-deficient Derivative Reveals the Role of PDHC in the Fermentative Metabolism of Glucose*. *J. Biol. Chem.* **2010**, *285*, 31548−31558.

(23) Kim, H. J.; Jeong, H.; Lee, S. J. Glucose Transport through N-Acetylgalactosamine Phosphotransferase System in *Escherichia coli* C Strain. *J. Microbiol. Biotechnol.* **2022**, *32*, 1047−1053.

(24) Zhu, Y.; Du, S.; Yan, Y.; Pan, F.; Wang, R.; Li, S.; Xu, H.; Luo, Z. Systematic engineering of Bacillus amyloliquefaciens for efficient production of poly-γ-glutamic acid from crude glycerol. *Bioresour. Technol.* **2022**, *359*, No. 127382.

(25) Xia, H. H.; Zhu, N. Q.; Wang, Z. W.; Chen, T. In *PROCEEDINGS OF THE 2012 INTERNATIONAL CONFERENCE ON APPLIED BIOTECHNOLOGY (ICAB 2012), VOL 1*; Zhang, T. C.; Ouyang, P.; Kaplan, S.; Skarnes, B., Eds.; International Conference on Applied Biotechnology (ICAB), 2014; Vol. *249*.

(26) Dauner, M.; Bailey, J. E.; Sauer, U. Metabolic flux analysis with a comprehensive isotopomer model in Bacillus subtilis. *Biotechnol. Bioeng.* **2001**, *76*, 144−156.

(27) Akkermans, S.; Van Impe, J. F. Mechanistic modelling of the inhibitory effect of pH on microbial growth. *Food Microbiol.* **2018**, *72*, 214−219.

(28) Ojima, Y.; Komaki, M.; Nishioka, M.; Iwatani, S.; Tsujimoto, N.; Taya, M. Introduction of a stress-responsive gene, yggG, enhances the yield of l-phenylalanine with decreased acetic acid production in a recombinant *Escherichia coli*. *Biotechnol. Lett.* **2009**, *31*, 525−530.

(29) Chao, Y. P.; Liao, J. C. Metabolic responses to substrate futile cycling in *Escherichia coli*. *J. Biol. Chem.* **1994**, *269*, 5122−5126.

(30) Lee, H. J.; Kim, H.; Seo, J.; Na, Y. A.; Lee, J.; Lee, J.; Kim, P. Estimation of phosphoenolpyruvate carboxylation mediated by phosphoenolpyruvate carboxykinase (PCK) in engineered *Escherichia coli* having high ATP. *Enzyme Microb. Technol.* **2013**, *53*, 13−17.

(31) PENG, L.; Arauzo-Bravo, M. J.; Shimizu, K.; et al. Metabolic flux analysis for a ppc mutant *Escherichia coli* based on 13C-labelling experiments together with enzyme activity assays and intracellular metabolite measurements. *Fems Microbiol. Lett.* **2004**, *235*, 17−23.

(32) Hashiguchi, K.-i.; Kojima, H.; Sato, K.; Sano, K. Effects of an *Escherichia coli* ilvA mutant gene encoding feedback-resistant threonine deaminase on L-isoleucine production by Brevibacterium flavum. *Biosci., Biotechnol., Biochem.* **1997**, *61*, 105−108.

https://doi.org/10.1021/acsomega.3c07619
ACS Omega 2024, 9, 10276−10285